Plant Science 241 (2015) 151–163

Contents lists available at ScienceDirect

Plant Science

journal homepage: www.elsevier.com/locate/plantsci

Biochemical characterization of the novel *endo*-β-mannanase *At*Man5-2 from *Arabidopsis thaliana*

Yang Wang[a], Shoaib Azhar[b], Rosaria Gandini[a,c], Christina Divne[a,c], Ines Ezcurra[a], Henrik Aspeborg[a,*]

[a] From KTH Royal Institute of Technology, School of Biotechnology, Division of Industrial Biotechnology, AlbaNova University Center, 106 91 Stockholm, Sweden
[b] From Wallenberg Wood Science Center, Department of Fiber and Polymer Technology, KTH Royal Institute of Technology, 100 44 Stockholm, Sweden
[c] From Karolinska Institute, Department of Medical Biochemistry and Biophysics, Scheelelaboratoriet, Scheeles väg 2, 17177 Stockholm, Sweden

ARTICLE INFO

Article history:
Received 4 April 2015
Received in revised form 8 September 2015
Accepted 2 October 2015
Available online 22 October 2015

Keywords:
Glycoside hydrolase
GH5
endo-β-1,4-Mannan hydrolase
Cell wall
Mannan polysaccharides/oligosaccharides

ABSTRACT

Plant mannanases are enzymes that carry out fundamentally important functions in cell wall metabolism during plant growth and development by digesting manno-polysaccharides. In this work, the Arabidopsis mannanase 5-2 (*At*Man5-2) from a previously uncharacterized subclade of glycoside hydrolase family 5 subfamily 7 (GH5_7) has been heterologously produced in *Pichia pastoris*. Purified recombinant *At*Man5-2 is a glycosylated protein with an apparent molecular mass of 50 kDa, a pH optimum of 5.5–6.0 and a temperature optimum of 25 °C. The enzyme exhibits high substrate affinity and catalytic efficiency on mannan substrates with main chains containing both glucose and mannose units such as konjac glucomannan and spruce galactoglucomannan. Product analysis of manno-oligosaccharide hydrolysis shows that *At*Man5-2 requires at least six substrate-binding subsites. No transglycosylation activity for the recombinant enzyme was detected in the present study. Our results demonstrate diversification of catalytic function among members in the Arabidopsis GH5_7 subfamily.

1. Introduction

Mannan polysaccharides are non-crystalline hemicelluloses that exist in various organisms such as bacteria, fungi and plants. Higher-plant mannans are involved in several biological processes during cell wall degradation and modification [1,2], but also serve as raw biopolymers that are widely used in food industry, paper pulping, and biofuel production [3–5]. As structural cell-wall components, mannan polysaccharides are suggested to cross-link or coat cellulose microfibrils, and to form linkages to other hemicelluloses and lignin, although mannan may also serve as carbohydrate reserves in seeds and tubers [6]. All mannan types contain a backbone of β-1,4-linked mannose units, whereas β-1,4-linked mannosyl and glucosyl residues can presumably be randomly distributed in the backbones of heterogeneous mannans [7]. Additionally, mannose residues in the main chain can be grafted by α-1,6-linked galactose units forming side chains.

Based on the main-chain composition and the presence or absence of galactose side chains, mannan polysaccharides are typically classified into four major groups: pure mannans, glucomannans, galactomannans, and galactoglucomannans. In the model plant Arabidopsis, mannan polysaccharides are present as minor components in most cell types [8–11]. Glucomannan is the mannan polysaccharide found in the Arabidopsis stem and the seed mucilage [8,12], but whether other types of mannans exist in Arabidopsis tissues is currently not known [8,9,13]. Galactomannans are commonly found in seed endosperms from various plants but have not yet been found in Arabidopsis endosperm tissue [14].

Mannan-active enzymes play a key role in the natural recycling of biomass, and in the growth and development of plants [15]. They also serve as valuable biotechnological tools in industrial applications that utilize mannans [16,17]. Endo-acting β-mannanases (MANs) cleave the internal glycosidic bonds of the β-1,4-linked backbone of various mannans, and they constitute the principal enzymes involved in mannan depolymerization and/or modification. Based on protein sequence similarity, MANs characterized to date belong to either of the glycoside hydrolase (GH) families 5, 26 or 113, as classified according to the CAZy (www.cazy.org) database of carbohydrate-active enzymes [18]. Enzyme members of these GH families share a common three-dimensional (3D) fold known as the $(\beta/\alpha)_8$ barrel, or TIM barrel fold, and a similar catalytic machinery that hydrolyzes glycosidic bonds by retention of

* Corresponding author. Fax: +46 8 5537 8468.
E-mail address: henrik.aspeborg@biotech.kth.se (H. Aspeborg).

http://dx.doi.org/10.1016/j.plantsci.2015.10.002

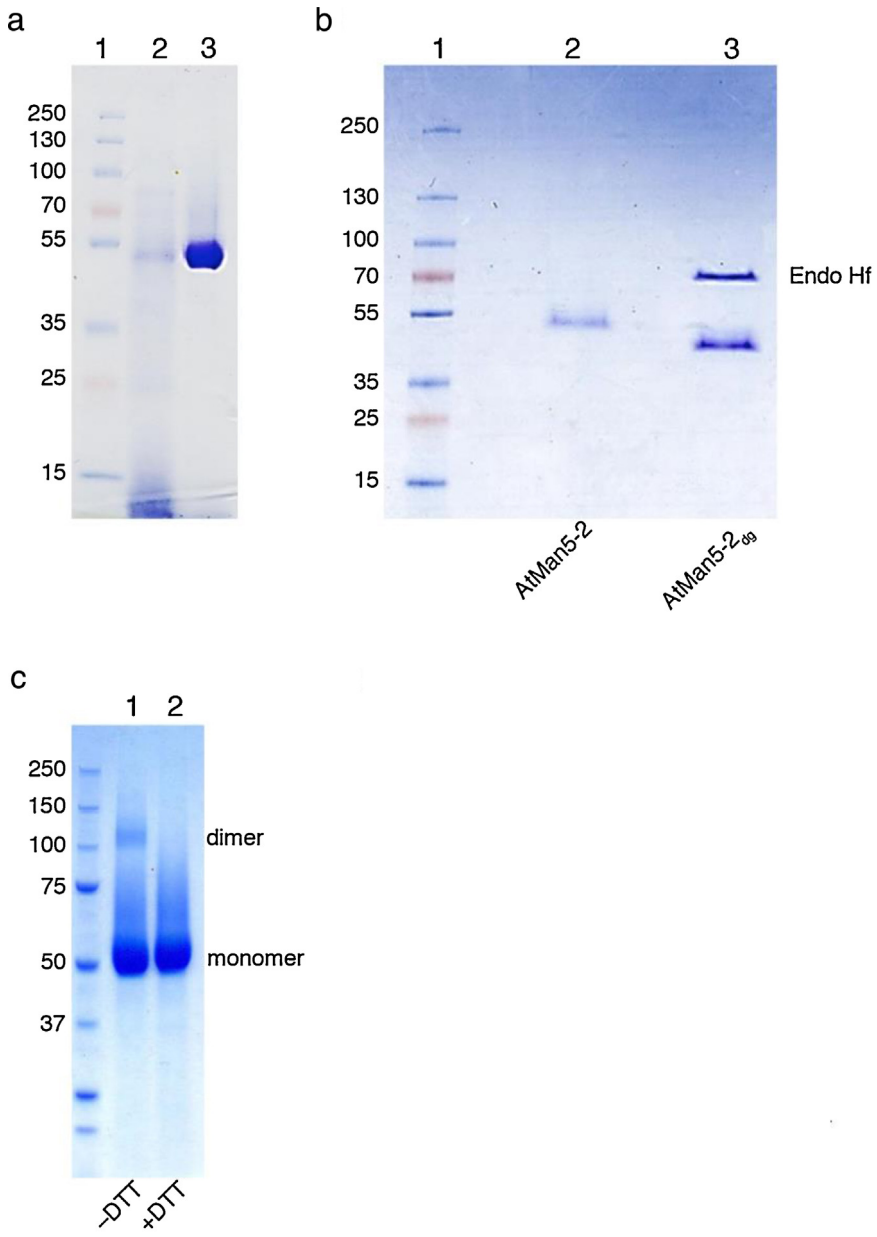

Fig. 1. (a) SDS-PAGE analysis of *At*Man5-2. Lanes: (1), protein molecular weight markers (PageRuler Plus, Thermo Scientific); (2), culture supernatant; and (3), IMAC-purified protein. (b) Analysis of de-glycosylation of *At*Man5-2 using Endo H_f. Lanes: (1), protein molecular weight markers (PageRuler Plus, Thermo Scientific); (2), glycosylated *At*Man5-2 before Endo H_f treatment; and (3), de-glycosylated *At*Man5-2 after Endo H_f treatment. (c) The effect of reducing agents on the oligomeric state of *At*Man5-2 analyzed by SDS-PAGE. Lanes (1), protein molecular-weight markers (Precision Plus, BioRad); (2), without DTT; and 3, with DTT.

configuration at the anomeric carbon, *i.e.*, a double-displacement (S_N1) mechanism [19,20]. An inherent ability of many retaining glycoside hydrolases is to catalyze the "reverse" reaction whereby a sugar moiety is used as an acceptor rather than a water molecule during the deglycosylation step (the second step of the retaining reaction) leading to the formation of a new glycosidic bond, *i.e.*, transglycosylation. Indeed, many microbial MANs and several plant MANs have been reported to exhibit both *endo*-hydrolytic and transglycosylation activity [21,23–26].

All sequenced genomes of higher plants contain genes coding for GH5 subfamily 7 (GH5_7) MANs [25,27] and a phylogenetic analysis of plant GH5_7 members revealed two principal clades of MANs [25]. Enzymatically characterized enzymes from tomato (*Solanum lycopersicum*, previously *Lycopersicon esculentum*), soybean (*Glycine max*), thale cress (*Arabidopsis thaliana*), barley (*Hordeum vulgare*) and coffee (*Coffea arabica*) are represented in clade 2 [21,24,25,28,29], whereas the only characterized enzyme in clade 1 is the *Populus trichocarpa Ptr*MAN6 [30]. It is not clear why plants need multiple forms of MANs, but one reason may be that the isoenzymes have evolved to exhibit different activities towards the various mannan substrates existing in plants.

To investigate the extent of catalytic diversification of plant GH5_7 enzymes, Arabidopsis provides an excellent plant model since its genome features seven full-length genes coding for MANs. Thus far, only a single characterized Arabidopsis MAN has been reported, namely the *A. thaliana* mannanase 1 (*At*Man5-1). *At*Man5-1 belongs to clade 2, and was shown to hydrolyze carob galactomannan, konjac glucomannan, spruce galactoglucomannan (sGGM) and mannopentaose (M5), as well as generating transglycosylation products [25]. Another Arabidopsis MAN, *A. thaliana* mannanase 2 (*At*Man5-2; locus At2g20680), belongs to clade 1 of the GH5_7 phylogenetic tree, and seed germination transcript

profiling has suggested a role for the enzyme in this process [31]. However, in contrast to the other MAN genes expressed in germinating seeds (*AtMan5-5*, *AtMan5-6* and *AtMan5-7*), the T-DNA insertion mutant of *AtMan5-2* did not affect the germination time course, indicating that the function of *At*Man5-2 is different from that of the other MANs associated with seed development [31].

In order to shed light on the function and catalytic properties of *At*Man5-2, we have produced heterologously *At*Man5-2 as a functional enzyme in *Pichia pastoris*. *At*Man5-2 is the first enzyme to be characterized in this subclade of the GH5_7 clade 1 enzymes, which are here shown to feature an unusual +1 substrate binding subsite and two conserved cysteine (Cys) residues in the C-terminal region. When comparing the catalytic properties of *At*Man5-2 to those of the previously reported *At*Man5-1, we observe distinct differences in the substrate specificity between the two enzymes representing the two major evolutionary branches of plant GH5_7 MANs. This work reports, for the first time, on the catalytic diversification of plant MAN paralogs.

2. Materials and methods

2.1. Cloning, recombinant protein production and protein purification

To adopt the nomenclature of Arabidopsis GH5_7 MANs, the enzyme encoded by the gene identified as At2g20680 (*AtMAN2*) was named *At*Man5-2 [25]. The plasmid containing the full-length cDNA sequence encoding *At*Man5-2 was obtained from RIKEN [32,33]. A gene construct containing the catalytic domain (K35 to P433) of *At*Man5-2 without the putative signal peptide, was amplified by PCR using Phusion™ High-Fidelity Polymerase (Finnzymes) and optimized primers (forward primer: ATTATTGCGGCCGCCAAAACGGAGGGCGAG; reverse primer: GGCGGCTCTAGATGTGGTCTATGGGAACAC). The gene was cloned into the pPICZα C vector (Life Technologies) to generate a construct including the *Saccharomyces cerevisiae* α-factor secretion signal for secreted expression, and a C-terminal His_6-tag for convenient protein purification by immobilized metal affinity chromatography (IMAC). The identity of the target gene was verified by DNA sequencing (Eurofins MWG Operon). To produce the secreted target protein, *P. pastoris* SMD1168H transformed with the recombinant plasmid was grown as described for *At*Man5-1 in our previous work [25].

Recombinant His_6-tagged *At*Man5-2 was purified by IMAC using a HiTrap IMAC FF column (GE Healthcare) equilibrated with 20 mM sodium phosphate, 0.5 M sodium chloride, 5 mM imidazole, pH 7.4 (buffer A) mounted on an ÄKTA purifier system (GE Healthcare Life Sciences). The culture supernatant was loaded onto the column and washed with buffer A, after which linear gradient elution of 5–500 mM imidazole was performed in 20 mM sodium phosphate buffer including 0.5 M sodium chloride (pH 7.4). The purity and molecular mass of the recovered protein was evaluated using SDS-PAGE analysis (12% precast polyacrylamide gels, BIO-RAD, U.S.A.). The protein was incubated in the presence of reducing agents and heated at 95 °C for 5 min before loading on a gel. Protein concentration was determined by Bradford assay [34] using the BioRad Protein Assay Kit (Sweden). To confirm the identity of the purified protein, a single protein band with the expected size was cut out from the gel, digested by trypsin and identified by mass spectrometry (Science for Life Laboratory, Sweden).

2.2. Deglycosylation and analysis of the oligomeric state

Deglycosylation of recombinant *At*Man5-2 was performed by treating the protein with Endoglycosidase H_f (Endo H_f; New England BioLabs) following the manufacturer's instructions, and the result was analyzed by SDS-PAGE. To investigate whether reducing agents affect the oligomeric state of the *At*Man5-2, the purified protein was incubated in the presence or absence of 50 mM dithiotreitol (DTT), and heated at 75 °C for 7 min, followed by SDS-PAGE analysis.

2.3. Biochemical characterization

The hydrolytic activity of *At*Man5-2 was determined by quantifying the amount of reducing sugar released using the 3,5-dinitrosalicylic acid (DNS) reducing sugar assay [35], as described earlier [25]. One unit of MAN activity was defined as the amount of enzyme required to release reducing sugar equivalents to 1 μmol of mannose per min under the given conditions. The assay mixtures contained mannan poly- or oligosaccharides (all except sGGM were from Megazyme) and 0.2–1.9 μM *At*Man5-2 in 50 mM sodium acetate buffer. To determine the temperature profiles, thermostability of activity as well as effect of glycosylation and metal ions on *At*Man5-2 activity, activity assays were performed using 3 mg/mL konjac glucomannan in 50 mM sodium acetate buffer (pH 5.5) for 30 min.

The pH profile was determined using different 50 mM buffers: sodium formate pH 3.0–4.5; sodium acetate, pH 4.5–5.5; sodium citrate, pH 5.5–6.0; and sodium phosphate, pH 6.0–7.0. The temperature profile was determined within the temperature range 0–45 °C in steps of 5 °C. To determine thermostability of activity, aliquots of enzyme (1.5 μM) were incubated at different temperatures in the range 15–45 °C in steps of 10 °C. Following incubation, the residual activity was measured at different time points, *i.e.*, 30, 60, 120 and 240 min.

To assess the effects of freeze–thawing, enzyme samples were stored at −20 °C, followed by measuring the residual activity at different time points, *i.e.*, 1, 2, 4 and 22 h. To analyze the effect on activity of treating *At*Man5-2 with Endo H_f to remove surface-attached *N*-glycans, the enzyme was incubated in the absence (control) or presence of Endo H_f at 37 °C for 2 h, immediately followed by activity measurements.

To analyze the effect of reducing agents on the activity, the enzyme was incubated in the presence of reducing agent, *i.e.*, 1, 10 and 50 mM DTT/β-mercaptoethanol (βMe) in 20 mM sodium phosphate buffer (pH 7.4) at room temperature for 1 h. Following incubation with reducing agent, the residual activity was determined using a reaction mixture containing 4 mg/mL konjac glucomannan at the given concentration of reducing agent at optimal reaction conditions for 4 h, *i.e.*, sodium acetate buffer (50 mM, pH 5.5) and 25 °C. Protein samples without reducing agent were used as controls and treated identically to those containing reducing agent.

The influence of metal ions on *At*Man5-2 activity was analyzed for a range of chloride salts, *i.e.*, Ca^{2+}, Co^{2+}, Fe^{3+}, Li^{+}, Mg^{2+} and Ni^{2+}. *At*Man5-2 was incubated with 5 mM EDTA and EGTA at room temperature for 1 h, and washed with 50 mM sodium acetate buffer (pH 5.5) using 30 kDa cutoff Amicon Ultra centrifugal filters (Millipore). Then, metal salts were added to the enzyme solutions to a final concentration of 5 mM, and the activity measured after 30 min incubation. Blank controls were prepared in the same way as the samples but using the 20 mM sodium phosphate buffer instead of enzyme. To determine and compare the activity of *At*Man5-2 on different mannan-polysaccharides; carob galactomannan (1.0–5.0 mg/mL), konjac glucomannan (1.5–6.0 mg/mL) and sGGM (2.0–6.0 mg/mL) were incubated with enzymes in sodium acetate buffer (50 mM, pH 5.5) at 25 °C. Due to the polydisperse nature of the mannan substrates used in the reactions, the apparent Michaelis constant K_m was expressed in mg/mL. The apparent k_{cat} was calculated as the maximum catalytic formation

of product (μmol) per unit enzyme (μmol) per unit time (s) under saturating substrate condition.

2.4. Product analysis from mannan-polysaccharides and oligosaccharides

To analyze the hydrolysis products, *At*Man5-2 was incubated with 1 mg/mL mannan polysaccharides (carob galactomannan, konjac glucomannan, guar gum, sGGM and carboxymethyl cellulose) or 1 mM manno-oligosaccharides (mannotriose, M3; mannotetraose, M4; mannopentaose, M5; mannohexaose, M6; and cellohexaose, C6) at 25 °C for 48 h. The transglycosylation activity of *At*Man5-2 was investigated under conditions that favor transglycosylation, *i.e.*, high concentrations of substrate and salt. For this purpose, enzyme samples (1.9 μM) were incubated with 5 mM M5/M6 with or without 1 M NaCl at 25 °C for 24 h. Hydrolysis products were identified and analyzed by high-performance anion-exchange chromatography with pulsed amperometric detection (HPAEC-PAD) as reported previously [25].

2.5. Protein sequence analysis, homology modeling and ligand docking

Protein sequences used for bioinformatics analyses were retrieved from Phytozome version 10 (http://phytozome.jgi.doe.gov). Multiple sequence alignment was performed using ClustalW2 (http://www.ebi.ac.uk/Tools/msa/clustalw2). To analyze conserved residues in *At*Man5-2 and the related plant GH5_7 enzymes in the *At*Man5-2 subclade, a multiple sequence alignment was performed using 38 protein sequences, and the data presented by WebLogo analysis (http://weblogo.threeplusone.com/create.cgi). Sequence motifs for N-linked glycosylation were predicted by NetNGlyc 1.0 Server (http://www.cbs.dtu.dk/services/NetNGlyc/), and phosphorylation sites were predicted by NetPhos 2.0 Server (http://www.cbs.dtu.dk/services/NetPhos/).

Homology models of *At*Man5-2 were generated automatically using *RaptorX* [36], *PHYRE2* [37] and *SWISS-MODEL* [38]. The geometry of the homology models was analyzed using *MolProbity* (http://molprobity.biochem.duke.edu; [39]). All models had acceptable geometry, but the model generated by *SWISS-MODEL* performed best with respect to coarse and fine packing quality as determined by *WHAT IF* [40]. To analyze the possible sugar-binding subsites in *At*Man5-2, an extended manno-oligosaccharide was docked manually to the binding cleft of the *SWISS-MODEL* homology model. Modeling of the oligosaccharide was guided by sugar binding in the crystal structures of: *Trichoderma reesei* (anamorph of *Hypocrea jecorina*) *Tr*Man5A in complex with M2 bound to subsites +1 and +2 (PDB code 1QNR; [41]); *Rhizomucor miehei Rm*Man5B E202A variant in complex with mannotriose (M3) bound to subsites −1, +1 and +2 (PDB code 4LYQ; [42]); and *Thermomonospora fusca Tf*Man in complex with M3 bound in subsites −4, −3 and −2 (PDB code 3MAN; [43]). More precisely, the three crystal structures and the

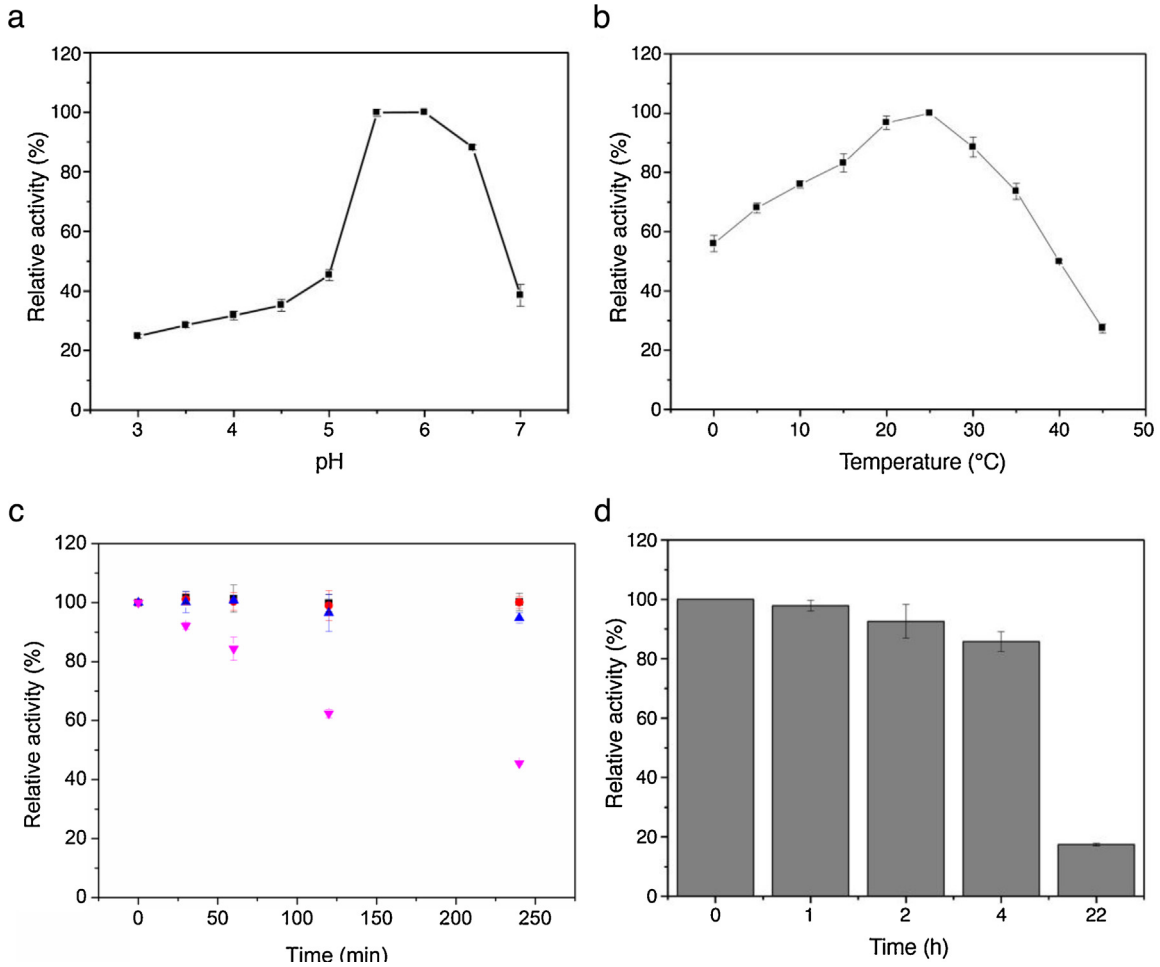

Fig. 2. Optimum activity of *At*Man5-2 using konjac glucomannan as substrate as a function of pH (a), and temperature (b). For calculation of residual activity, the optimum activity was set as 100%. (c) Thermostability of *At*Man5-2 activity using konjac glucomannan as substrate as a function of temperature and time: 15 °C (black squares); 25 °C (red circles); 35 °C (blue triangles); and 45 °C (pink inverted triangles). For calculation of residual activity, the activity at $t = 0$ was set as 100%. (d) Freeze–thaw resistance of *At*Man5-2 activity. For calculation of residual activity, the activity without freeze thawing was set as 100% activity. Time is the freezer storage time.

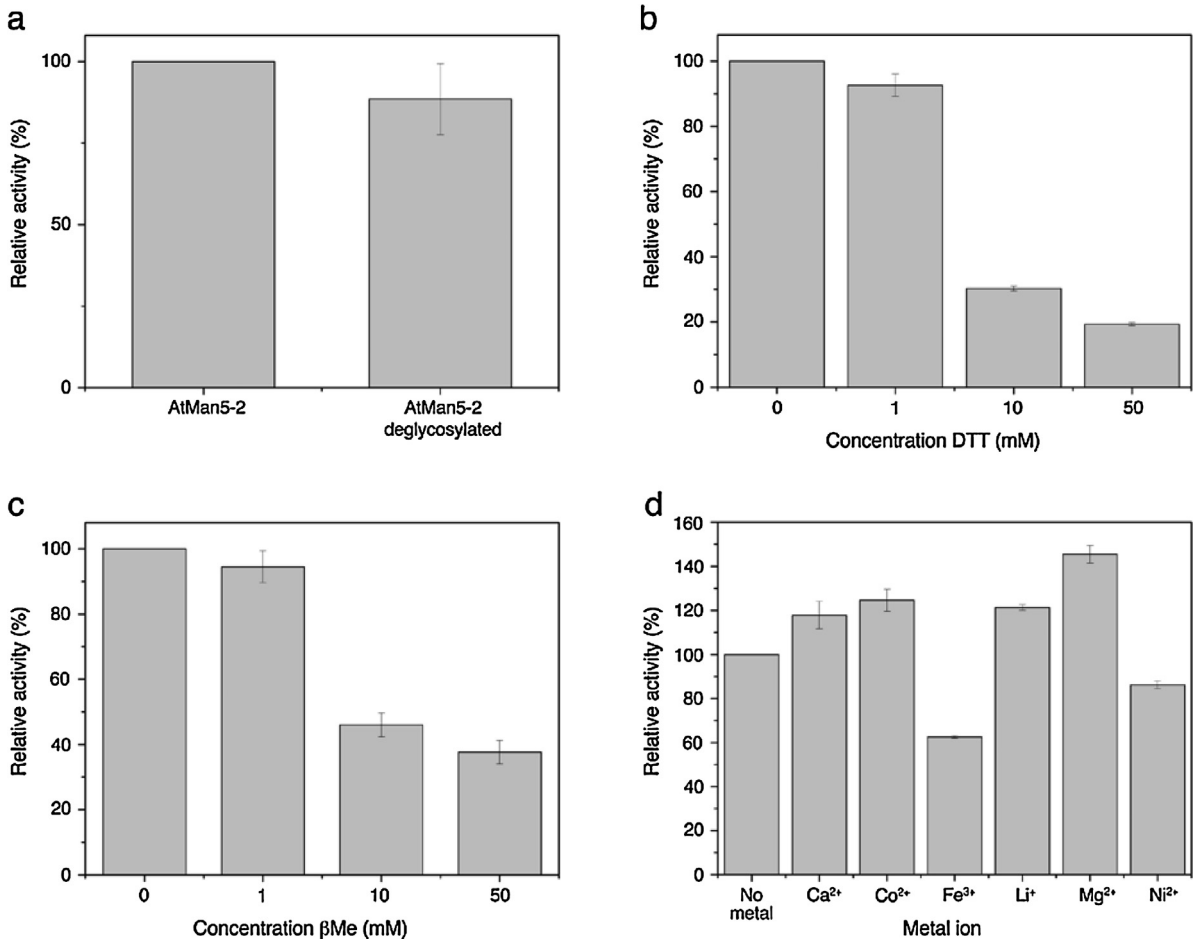

Fig. 3. (a) The effect of N-linked glycans on *At*Man5-2 activity. Glycosylated *At*Man5-2 was used as control, and the activity of *At*Man5-2 before Endo H_f treatment was set to 100%. The effect of reducing agents on *At*Man5-2 activity are shown for (b) DTT and (c) βMe where residual activity was calculated as a percentage of the activity observed in the absence of reducing agent (100% activity in the absence of reducing agent). (d) The effect of various metal ions on *At*Man5-2 activity with the activity in the absence of added metal ions corresponding to 100% activity. For all experiments, konjac glucomannan was used as substrate.

theoretical *At*Man5-2 model were superimposed and the sugars bound to the individual subsites in the experimental crystal structures were adjusted manually to optimize the fit of the sugars in the predicted subsites of the *At*Man5-2 model. Based on the structure of *Rm*Man5B with bound M3 [42], the mannose in subsite −1 was modeled as a 1*S*5 skew boat in the *At*Man5-2 model.

2.6. Analysis of expression and upstream sequences

The expression of the *AtMan5-2*, *AtMan5-5*, and POPTR_0013s13400 genes was investigated using the public microarray database BAR eFP [44,45]. Upstream promoter sequences (1500 bp from ATG) of *AtMan5-2* orthologs were retrieved from Phytozome. De novo motif analysis was performed by using MEME (http://meme.ebi.edu.au/meme/index.html [46]).

3. Results and discussion

3.1. Protein production and purification

The catalytic domain of *At*Man5-2 carrying a C-terminal His_6-tag was successfully produced in *P. pastoris* SMD1168H cells, and purified to homogeneity with a yield after IMAC of 16 mg/L. The recombinant fusion protein including the *At*Man5-2 catalytic domain, consisting of 399 amino-acid residues, a *c-myc* epitope, a His_6-tag and an additional peptide sequence in between the signal sequence processing sites and the start of the catalytic domain migrates on SDS-PAGE gels as a distinct band with an approximate molecular mass of 50 kDa (Fig. 1a). Mass spectrometry (MS) analysis identified 30 unique peptides that matched the amino acid sequence of *At*Man5-2 (Supplemental Fig. S1). The MS analysis also revealed phosphorylation of Ser81, although only approximately 8% of the peptides carrying Ser81 were identified as phosphopeptides. Phosphorylation of *At*Man5-2 in *Pichia* indicates that the protein has potential to be phosphorylated also *in planta*. Treatment with Endo H_f to remove N-linked glycans resulted in a decrease in molecular weight (Fig. 1b), thus confirming that recombinant *At*Man5-2 is generated by *P. pastoris* as a glycoprotein. The apparent molecular weight of the deglycosylated AtMan5-2 is estimated to be around 5 kDa lower than the calculated molecular weight of approximately 50.7 kDa.

The first 28 amino acids were not included in the gene construct since these are predicted to constitute a signal peptide. Furthermore, the *C*-terminus of the produced protein appears to be intact since the C-terminal His_6-tag was positively identified using a His probe and Western Blot analysis (data not shown). The low coverage for the C-terminal region by MS analysis is therefore not due to prematurely terminated translation or proteolytic cleavage. Thus, the aberrant migration of AtMan5-2 on SDS-PAGE cannot be explained by truncation, but rather, may be due to factors such as protein sequence composition, posttranslational modifications and/or structural features that may influence protein electrophoresis migration.

No support for glycosylation was obtained from the MS analysis, because the peptides containing the two predicted glycosylation sites were not identified. Glycosylation was also reported for the *Pichia*-produced *At*Man5-1 enzyme, although the recombinant *At*Man5-1 appears to be more extensively glycosylated compared with the heterologously produced *At*Man5-2 [25]. Glycosylation of recombinant proteins produced in heterologous eukaryotic hosts will often differ from the native protein. Consequently, we do not know if N-glycans are attached to the *At*Man5-2 and *At*Man5-1 proteins *in planta*, but glycosylation of a poplar MAN has been observed [30], so it seems reasonable to expect that these *Arabidopsis* enzymes are native glycoconjugates. Under non-reducing conditions, *At*Man5-2 migrates as two bands on the SDS-PAGE gel (Fig. 1c, lane 2), one major band corresponding to the 50 kDa monomer and one minor band with the apparent mass of a dimer. Under reducing conditions, however, only the monomeric band is present (Fig. 1c, lane 3) suggesting that intermolecular disulfide bonds may mediate dimer formation. To further investigate possible *At*Man5-2 oligomerization, size exclusion chromatography (SEC) analysis was performed, and using this method only the monomer was observed in solution (Supplemental Fig. S2). There is a slight leading shoulder in the gel-filtration profile of *At*Man5-2 that may indicate traces of a dimeric species. Thus, *At*Man5-2 can exist as a dimer, but the predominant form in solution is the monomer.

3.2. Determination of pH and temperature dependence of activity and thermostability of activity

The hydrolytic activity of *At*Man5-2 was studied as a function of temperature and pH using konjac glucomannan as substrate. *At*Man5-2 displayed maximum activity at pH 5.5–6.0 with an apparent optimal temperature at 25 °C (Fig. 2a,b). The activity was also examined as a function of temperature and time (Fig. 2c). After four hours of incubation at temperatures up to 35 °C, *At*Man5-2 retained 90–100% of the initial activity. At 45 °C, however, the residual activity remaining after 4 h was 45%. Freeze-thawing was also found to affect *At*Man5-2 activity resulting in only 20% residual activity after 22 h incubation at –20 °C (Fig. 2d). The optimal pH for *At*Man5-2 activity is similar to the apparent pH optima reported for the *Pichia*-produced *At*Man5-1 [25] and other characterized plant MANs [24,28]. The two Arabidopsis GH5 MANs also show similar thermostability of activity, although the optimal temperature for activity was 10 °C lower for *At*Man5-2 compared with *At*Man5-1.

3.3. Influence of glycosylation, reducing agents and metal ions on activity

Next we investigated whether the observed glycosylation could affect catalysis. The influence of glycosylation on *At*Man5-2 activity was assessed by removing N-linked glycans using Endo H_f. No significant decrease in activity was observed after deglycosylation at 37 °C for 2 h (Fig. 3a), and this is in contrast to *Ptr*MAN6 where *N*-glycosylation was reported to be essential for catalytic activity [47]. Nevertheless, recombinant *Le*MAN4a from tomato and *At*Man5-1 were catalytically active although generated in *Escherichia coli* [24,25], so plant MAN activities seem to be diversely affected by protein glycosylation. Contrary to deglycosylation, addition of the reducing agents DTT and βMe significantly reduced *At*Man5-2 activity (Fig. 3b,c). Treatment with 50 mM DTT and βMe caused relative activity decreases of approximately 80% and 60%, respectively. Effects of various metal ions known to affect MAN activity were tested and these chemicals affected *At*Man5-2 activity to varying degree (Fig. 3d). While Mg^{2+} enhanced the relative activity, Ni^{2+} and Fe^{3+} reduced the activity to some extent, other cations showed marginal effects on activity. The precise mechanism of action for these divalent cations is not clear, but most likely they play a role by stabilizing local structure critical for activity as seen for an actinomycetes MAN [48].

3.4. Determination of kinetic constants for manno-polysaccharides

The kinetic parameters were determined for the natural mannan polysaccharides: carob galactomannan, konjac glucomannan and sGGM (Table 1). Amongst the substrates that were tested, konjac glucomannan displayed the highest V_{max} (6.7 U/mg), whereas lower maximal velocities were obtained with carob galactomannan (2.5 U/mg) and sGGM (1.7 U/mg). sGGM showed the lowest Michaelis constant (sGGM, K_m = 0.5 mg/mL; konjac glucomannan, K_m = 1.3 mg/mL; carob galactomannan, $K_m \sim$ 12.8 mg/mL). The activity on guar gum galactomannan was too low to be accurately measured. When comparing the obtained catalytic properties of *At*Man5-2 with those determined for *At*Man5-1 [25] some differences are noted. While *At*Man5-2 seems to have a preference for substrates with a mannan backbone containing glucose, *At*Man5-1 is able to hydrolyze carob galactomannan, konjac glucomannan and sGGM at comparable efficiencies. These results suggest glucomannan may be the *in vivo* substrate for *At*Man5-2.

3.5. Product patterns from manno-polysaccharides and oligosaccharide hydrolysis

To further elucidate the *At*Man5-2 enzymatic mode of action product patterns of hydrolysis using manno-polysaccharides and oligosaccharides were analyzed using HPAEC-PAD. The major mannan oligosaccharide products from carob galactomannan hydrolysis were mannobiose (M2) and M4, as well as a smaller peak identified as M5 (Fig. 4a). Hydrolysis of konjac glucomannan generated mainly M2 and M4 with minor amounts of M3 and M5, and for sGGM, weak product traces of M2, M4 and M5 were detected. With guar gum galactomannan as substrate, only a weak trace of M4 was produced. Both *At*Man5-2 and *At*Man5-1 showed negligible activity toward the highly branched guar gum galactomannan, but the hydrolytic cleavage profiles obtained for the other substrates were divergent. For instance, *At*Man5-1 produced M2, M3 and significant amounts of GM3 from carob galactomannan, but M2 and M3 from konjac glucomannan with M2 being the principal product [25]. Unidentified and overlapping peaks observed in the experiments probably represent short glucomanno-oligosaccharides or branched galactomanno-oligosaccharides.

Furthermore, the present study revealed that *At*Man5-2 was not able to degrade carboxymethyl cellulose (CMC), nor C6, M3, M4 and M5 (data not shown), whereas M6 was hydrolyzed to give M2, M3 and M4, with M3 as the predominant species (Fig. 4b). The absence of reaction products released from M3-M5 incubated with the *At*Man5-2 revealed the requirement of at least six substrate-binding subsites. Although the hydrolysis product patterns of M6 are similar for *At*Man5-2 and *At*Man5-1, the latter enzyme was also able to degrade M5 generating M2 and M3. This suggests that both enzymes have at least six sugar-binding subsites. The affinity of the individual subsites differ to generate catalytic diversification between these two Arabidopsis GH5 MANs.

Since *in vitro* transglycosylation activity has been reported for several plant MANs [21,24,25], attempts were made to find evidence for transglycosylation. The absence of manno-oligosaccharides of higher degree of polymerization (DP) than M6, was interpreted as no significant transglycosylation had occurred even at high substrate concentration or with the addition of salt [24]. However, any transient transglycosylation products hydrolyzed by *At*Man5-2 may not have been measurable by the method. On the other hand, transglycosylation products were

Table 1
Apparent kinetic parameters of AtMan5-2 on manno-polysaccharides.

Manno-polysaccharides	V_{max} (U/mg)	K_m (mg/mL)	k_{cat} (s^{-1})	k_{cat}/K_m (s^{-1} mg^{-1} mL)
Carob galactomannan	2.5 ± 0.08	12.8 ± 0.38	2.1 ± 0.06	0.2 ± 0.0001
Konjac glucomannan	6.7 ± 0.14	1.3 ± 0.04	5.7 ± 0.12	4.3 ± 0.05
Spruce galactoglucomannan	1.7 ± 0.06	0.5 ± 0.04	1.5 ± 0.05	2.8 ± 0.12

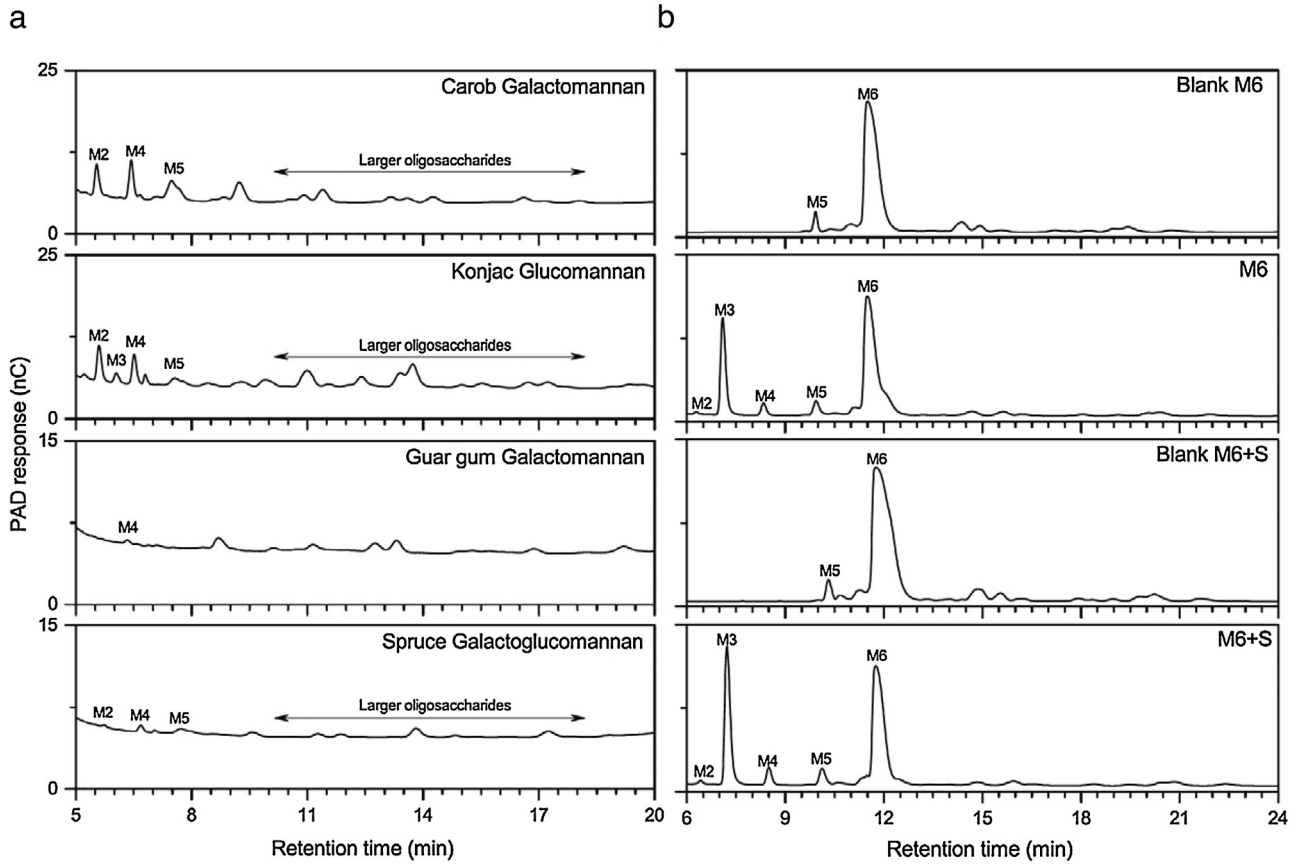

Fig. 4. (a) HPAEC-PAD oligosaccharide profiles following enzymatic treatment of different mannan poly- and oligosaccharides. (b) HPAEC-PAD profiles of mannohexaose (M6) and mannohexaose with increased substrate concentration and addition of salt (M6 + S). Mannopentaose (M5) was present as a contaminant in the M6 sample as shown in controls without enzyme (Blank M6) and (Blank M6 + S). M2, mannobiose; M3, mannotriose; M4, mannotetraose; M5, mannopentaose; M6, mannohexaose.

detected for recombinant *At*Man5-1 incubated with M5 and M6 under similar conditions favoring transglycosylation as used in the present study. The observed contrasting behavior of *At*Man5-2 and *At*Man5-1 likely illustrates different capacity to perform transglycosylation reactions and is yet another sign that these enzymes have evolved to function differently.

3.6. Protein sequence analysis

The *At*Man5-2 gene codes for 433 amino-acid residues with a putative *N*-terminal signal peptide (residues 1–28) for secretion. We have reported earlier that *At*Man5-2 and *At*Man5-5 belong phylogenetically to the same subclade of clade 1, one of the two major clades of plant GH5_7 MANs [25]. This implies that these proteins are closely related. A protein sequence alignment including the clade-1 MANs (*At*Man5-2, *At*Man5-5, and *Ptr*MAN6) and biochemically characterized clade-2 MANs (*At*Man5-1 and *Le*MAN4a) is shown in Fig. 5a. The sequences of *At*Man5-2 and *At*Man5-5 are indeed similar with 83% sequence identity.

Of the enzymes in clade 1, only *Ptr*MAN6 has been characterized biochemically, but this enzyme belongs to a different subclade of clade 1 [30,47]. The two glutamate residues performing the catalytic roles as acid/base (Glu215 in *At*Man5-2) and nucleophile (Glu335 in *At*Man5-2) are conserved in all aligned sequences (Fig. 5a). Other residues that are typically conserved among GH5 enzymes are found also in *At*Man5-2, *i.e.*, Arg96, His293, Tyr295 and Trp377. Plant MANs have been reported to be generated as glycoproteins [25,30], and in this study *At*Man5-2 was produced as a glycosylated recombinant protein by *P. pastoris*. There are two N-X-T/S sequence motifs for *N*-glycosylation in *At*Man5-2, ^{46}NGT^{48} and ^{169}NDS^{171}, of which the former exists in *At*Man5-2, *At*Man5-1 and *At*Man5-5, and the latter only in *At*Man5-2 and *At*Man5-5 (Fig. 5a). The Ser81 identified as being phosphorylated with MS was predicted as a potential phosphorylation site using NetPhos 2.0, although this software has not been trained using secreted phosphoproteins.

The fact that thiol-reducing agents affected the oligomeric state of *At*Man5-2 motivated a search for Cys residues in the protein sequences. *Ptr*MAN6 and its plant orthologs feature three conserved Cys residues in the C-terminal region: Cys448, Cys452 and Cys456 [47]. These Cys residues have been confirmed experimentally to play a role in dimerization of *Ptr*MAN6, and also to affect the enzyme's catalytic activity [30,47]. One of the Cys residues (Cys456 in *Ptr*MAN6) is present in *At*Man5-2 (Cys429) and *At*Man5-

a

```
AtMan5-1        -------MLN--ILPFFLFFLPFLIGNNRICVAVKTG---------------------- 28
LeMAN4a         -------MNNSIILIFVAILIIFPNEFSKPTRAFSNNN---------------------- 31
PtrMAN6         -MDTHKRVFGFKIIFLVSVFILLNESSKCSSSGVMDDEQFKTMVEEVDNHLPSSSSSQGV 59
AtMan5-2        MAAPTGNGPVIPILGFLTCVAFIYLSFGDLWFGLKTEGELA------------------- 41
AtMan5-5        -MVPTRNRPMLRILGFFICAAFIYLSFRDLWLNHKGKAKLG------------------- 40
                          *: :.    :
                          glycosylation site
AtMan5-1        ------------FVGRNGTCFVLNGEQVYLNGFNAYWMMTTAADTASKGRATVTTALRQA 76
LeMAN4a         ------------FVYTDGTHFALNGKSLYINGFNAYWLMYIAYDPST--RIKVTNTFQQA 77
PtrMAN6         YELNDVEEDEWLMVAKKGNQFVINDQPFYVNGFNTYWLMVFAADQST--RGKVTEVFQKA 117
AtMan5-2        ------------FVKRNGTCFVVDGKALYVNGWNSYWFMDHAVNDHS--RHRVSAMLEAG 87
AtMan5-5        ------------FVKRNGTCFVVDDKPLYVNGWNSYWFMDHAVDEHS--RNLVGEMLEAG 86
                            :*  .*.:*.::.: .*:**:*:**:*  * :  :  *  *   :. .
AtMan5-1        SAVGMNVARIWGFNEGDYIPLQISPGSYSEDVFKGLDFVVYEAGRFNIKLIISLVNNFED 136
LeMAN4a         SKYKMNVARTWAFSHGGSRPLQSAPGVYNEQMFQGLDFVISEAKKYGIHLIMSLVNNWDA 137
PtrMAN6         SSVGLSVCRTWAFNDGQWRALQKSPGVYDEDVFKALDFVVSEANKYKIRLILSLANNWDA 177
AtMan5-2        AKMGLTVCRTWAFNDGGYNALQISPGRFDERVFKALDHVIAEAKTHGVRLLLSLVNNLQA 147
AtMan5-5        AKMGLTVCRTWAFNDGGYNALQISPGRFDERVFQALDHVIAEARKHDVRLLLSLVNNLQA 146
                :   :.*.* *.*..*   .** :** :.* :*:.**.*: **  . ::*::**.** :
                                   glycosylation site
AtMan5-1        YGGRKKYVEWAG-----LDEPDE-FYTNSAVKQFYKNHVKTVLTRKNTITGRMYKDDPTI 190
LeMAN4a         FGGKKQYVEWAVQRGQKLTSDDD-FFTNPMVKGFYKNNVKVVLTRVNTITKVAYKDDPTI 196
PtrMAN6         YGGKAQYVKWGKASGLNLTSDDD-FFSHPTLRSYYKAHVKAVLNRVNTITNITYKDDPTI 236
AtMan5-2        YGGKTQYVNWAWQEGVGLSSSNDSFFFDPSIRRYFKNYLTVLLTRKNSLTGIEYRNDPTI 207
AtMan5-5        YGGKTQYVKWAWQEGVGLSSSNDSFFFDPSIRNYFKNYLKVLLTRKNSVTGIEYRNDPTI 206
                :**: :**:*.      * . :: *: .. :: ::*  :..:*.* *::*   *::****
                catalytic acid/base
AtMan5-1        FSWELINEPRCNDSTASNILQDWVKEMASYVKSIDSNHLLEIGLEGFYGESIPERTVYNP 250
LeMAN4a         LSWELINEPRCPSDLSGKTFQNWVLEMAGYLKSIDSNHLLEIGLEGFYGNDMRQ---YNP 253
PtrMAN6         FAWELMNEPRCTSDPSGDKLQSWITDMAVYVKSMDAKHLVEIGLEGFYGPSAPDRAQFNP 296
AtMan5-2        FAWELINEPRCMSDVSGDTLQDWINEMTAFIKSIDNKHLLTVGLEGFYGPSSPKKLTVNP 267
AtMan5-5        FAWELINEPRCTTDVSGKTLQDWIDEMTGFIKSIDDKHLLTVGLEGFYGPNSPKGLTVNP 266
                ::***:*****  . :.. :*.*: :*: ::**:* :**: :******* .  .    **
AtMan5-1        GGR-VLTGTDFITNNQIPDIDFATIHIYPDSWLPLQSSRTGEQDTFVDRWIGAHIEDCDN 309
LeMAN4a         NS--YIFGTNFISNNQVQGIDFTTIHMYPNQWLPGLT--QEAQDKWASQWIQVHIDDSK- 308
PtrMAN6         NSYATQVGTDFIRNHQVLGVDFASVHIYADSWISQTI--TDSHIQFTKSWMEAHIEDAEK 354
AtMan5-2        ERWASELGSDFVRNSDSPNIDFASVHIYPDHWFHDQG--FEEKLKFVVKWMLSHIEDGDK 325
AtMan5-5        EQWASQLGTDFVQNSNSSNIDFASVHIYPDHWFHNQT--FEEKLKFVVKWMQSHIEDGLK 324
                   *::*: * :  .:**:::*:*.: *:          :  :.  *:  **:*
                catalytic nucleophile
AtMan5-1        IIKKPLLITEFGKSSKYPGFSLEKRNKFFQRVYDVIYDSARAGGSCTGGVFWQLTTNRTG 369
LeMAN4a         MLKKPLLIAEFGKSTKTPGYTVAKRDNYFEKIYGTIFNCAKSGGPCGGGLFWQVLGQGMS 368
PtrMAN6         YLGMPVVFAEFGVSSKDPGYNSSFRDTLINTVYKTLLNSTKRGGSGAGSLLWQLFPDGTD 414
AtMan5-2        ELKKPVLFTEFGLSNLNKDYDPSQRDRFYRTIFDVIYKSAKRKRSGAGTLVWQFLIEGME 385
AtMan5-5        ELKKPVLFTEFGLSNQNKDYEPSQRDKFYRIIFDVVYKSAKRKKSGAGTLVWQLFMEGME 384
                 :  *::::*** *.   .:    *:   . :: .: ..::   .  * :.**.  :

AtMan5-1        LLGDGYEVFMQAGPNTTAQLIADQSSKLKNLKYPPLVTHSAE------------------ 411
LeMAN4a         SFDDGYQVVLQESP-STSRVILLQSLRLSKLS---------------------------- 399
PtrMAN6         YMDDGYAIVLSKSP-STTNIISLHSTRVAIVN--SMCSWKCKWGCKKRNPLEAFLYHDDL 471
AtMan5-2        GFNDDFGIVPWEQD-SIQRLMIEQSCRLSRITGRHLLDKKSIEMCSHRP----------- 433
AtMan5-5        TFNDDFGIVPHEQD-SIYKLMIEQSCRLGKVTGR-LKEQKLKELCSHRH----------- 431
                 :.*.: :.      :  .::  :* ::  :.
```

b

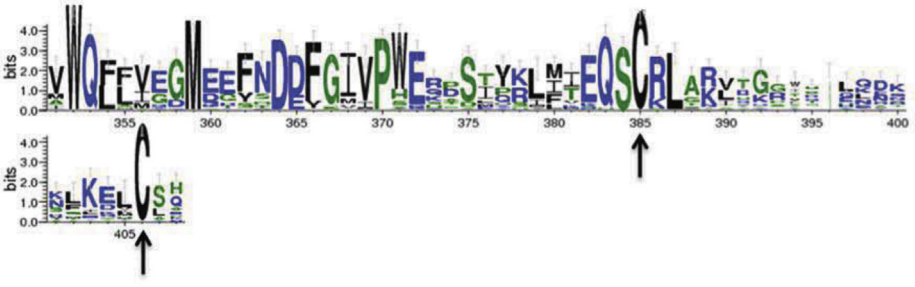

Fig. 5. (a) Protein sequence alignment including *At*Man5-2 (locus At2g20680, UniProtKB accession Q7Y223), and selected GH5_7 plant MANs from *A. thaliana* (*At*Man5-1, locus At1g02310, UniProtKB accession Q9FZ29; *At*Man5-5, locus At4g28320, UniProtKB accession Q9M0H6), *S. lycopersicum* (*Le*MAN4a, UniProtKB Q8L5J1) and *P. trichocarpa* (*Ptr*MAN6, UniProtKB accession B9IGV3). Two predicted glycosylation sites (^{46}NGT^{48} and ^{169}NDS^{171}) are shown and two catalytic glutamic acid residues are framed by squares. Arrows denote additional amino acids in GH5 members that are typically conserved. The arginine positioned at substrate binding site +2 is marked with a circle. (b) WebLogo analysis of the C-terminal region of a sequence-alignment using the amino acid sequences of *At*Man5-2 and 38 GH5_7 plant MANs belonging to the same subgroup as *At*Man5-2. Arrows highlight two highly conserved Cys residues.

5 (Cys427). We also identified a second Cys residue present in *At*Man5-2 (Cys410) and other members of this particular subclade (Fig. 5b). Possibly, these Cys residues have a functional role in *At*Man5-2 and closely related plant MANs. Interestingly, *Pichia*-produced recombinant *At*Man5-2 protein can also exist as dimers *in vitro* under non-reducing conditions, leading to a polydisperse protein solution consisting of monomers (main species) and dimers (minor species). Thus, it is conceivable that at least one of the Cys found in the C-terminal part may play a role in disulfide-mediated dimerization of *At*Man5-2, however, the function of dimerization is not clear. Although the enzyme activity can be inhibited by DTT and βMe, it is possible that these compounds interact directly with the active site to cause inhibition since the *At*Man5-2 monomer is the predominant species.

The function of the N-terminus in *At*Man5-2 is not known but may include a secretion signal. To further analyze the likelihood of a signal peptide at the N-terminus, the *At*Man5-2 sequence was analyzed using *SignalP 4.1* [49], *Phobius* [50], and *TOPCONS* [51]. Interestingly, *SignalP 4.1* fails to identify a signal peptide in *At*Man5-2 but reports a possible transmembrane helix, while both *Phobius* and *TOPCONS* report a strong signal for a transmembrane helix for residues 12–34 and 8–28, respectively. Hence, it is possible that *At*Man5-2 is a membrane-anchored enzyme, rather than secreted to the Arabidopsis cell wall.

3.7. Structural analysis of the theoretical homology models

Several homology models of *At*Man5-2 were generated. The closest homolog with known 3D structure is *Le*MAN4a (PDB code 1RH9; [52]; 43% sequence identity). The *Le*MAN4a template ends at Ser399 (Thr416 in *At*Man5-2) and therefore no trustworthy model could be generated for the C-terminal region where Cys410 and Cys429 are located. In many GHs, the *exo versus endo* modes of action is affected by the length of active-site loops [42,53]. This is true for *exo*-acting *Cm*Man5A and *Rm*Man5B where a long loop (378–412 in *Cm*Man5A; 354–392 in *Rm*Man5B) forms a double-steric block to exclude glycone subsites beyond subsite −1 [42]. In our model of *endo*-acting *At*Man5-2, and *Le*Man4a, this loop is shorter (380–394 in *At*Man5-2; 363–377 in *Le*Man4a), which creates an extended cleft that runs across one face of the molecule (Fig. 6a,b). Furthermore, a manno-oligosaccharide (M7) was docked in the *At*Man5-2 subsite +3 (aglycone side) to subsite −4 (glycone side) of the cleft that covers a length of 40 Å (Fig. 6c,d). With hydrolysis taking place between subsites −1 and +1, M7 is expected to generate mainly M3 and M4. The inability of *At*Man5-2 to hydrolyze manno-oligosaccharides shorter than M6, and M3 being the principal hydrolysis product from M6, is in agreement with the modeled *At*Man5-2 complex. Although mainly M3 is produced from M6, there are small amounts of M2 and M4 generated (Fig. 4b). This can be interpreted as four "negative" subsites (−4 to −1) and two of the possible "positive" subsites (+1 and +2) being used, thus implying four "negative" subsites rather than three, which is also supported by docking.

The "roof" of the cleft displays high sequence conservation with *Le*MAN4a whereas the "floor" is less well conserved, including the far aglycone end at subsite +3 where Arg269 and Trp270 lack counterparts in *Le*Man4a (Fig. 6e). Tyr105 and Phe387 may interact with a mannose in subsite −4, while Asp102 could interact in subsite −3 (Fig. 6f). In subsite −2, Asp389, Trp98, and possibly also Gln146 may provide interactions. In subsite −1, a distorted mannose may interact with Asn214 and Trp377 (Fig. 6g). The acid/base catalyst Glu215 and nucleophile Glu335 would be suitably positioned for bond cleavage at subsites +1/−1. In subsite +1, a modeled mannose unit may hydrogen bond to Glu252, while Leu145 could offer hydrophobic interactions (Fig. 6h). Trp299 may interact in subsite +2, while Arg269 and Trp270 are positioned in subsite +3 (Fig. 6i). GH5 MANs can accommodate both mannose and glucose in subsites −2 and +1 [54]. In our model, an axial O2 hydroxyl group appear favorable in subsites −2 and −1, which may suggest that these are mannose-recognition subsites rather than binding sites for glucose.

A tryptophan in subsite +1 in *Aspergillus niger* ManBK (Trp112) has been studied by mutagenesis [55]. The substitution Trp112→Gly resulted in a 13-fold increase in K_m and 26-fold decrease in k_{cat}, whereas for Trp112→Tyr the K_m value was unchanged and k_{cat} reduced 4.5-fold. This suggested that an aromatic residue is preferred in subsite +1. However, *At*Man5-2 subclade members have a leucine in this position (Leu145; Fig. 6h). The precise meaning of this discrepancy is unclear and needs further investigation by site-directed mutagenesis; however, hydrophobic interaction of a sugar with Leu is probably less favorable than a sugar-aromatic stacking interaction with the indole ring of a Trp.

Interactions in the aglycone subsites are thought to influence transglycosylation [22,56,57], especially an arginine in subsite +2 of fungal MANs [56]. In *Tr*Man5A, Arg171 in subsite +2 offers two hydrogen bonds to O2 and O3 of a mannose residue, as well as two ionic interactions with Glu205 (Glu252 in *At*Man5-2) [41]. The *Tr*Man5A variant R171K showed reduced transglycosylation and altered transglycosylation-product pattern [56]. Although this Arg is present also in *At*Man5-2 (Arg217), no transglycosylation was observed. Probably, transglycosylation is more complex and not due to any one single amino acid. Conceivably, weaker binding in subsite +1 due to Leu145 (Fig. 6h) may at least partly account for the loss of transglycosylation activity for *At*Man5-2.

3.8. Analysis of gene expression and conserved cis-regulatory motifs

Expression analyses by RT-PCR indicate that *AtMan5-2* is expressed in stem, roots, rosette leaves and germinating seeds, whereas *AtMan5-5* is weakly expressed in stem [58]. Moreover, *AtMan5-5* is highly expressed in mature dry seeds, whereas both genes are induced by germination [31]. Knockout analysis shows that *AtMan5-5*, but not *AtMan5-2*, is involved in seed germination [31]. Our extensive analysis of microarray expression databases indicates that *AtMan5-2* and *AtMan5-5* display opposing expression patterns during seed development and germination, where *AtMan5-2* is highly expressed during stages 3 to 7 in the developing seed, and *AtMan5-5* during stages 7–10 (Fig. 7a). Thus, the *AtMan5-2* transcript is predominant in the immature seed, whereas the *AtMan5-5* transcript is predominant in the mature dry seed. However, after 24 h imbibition, *AtMan5-2* expression is re-induced, and it becomes the predominant transcript again. Furthermore, *AtMan5-2* is highly expressed in the seed coat of heart stage embryo seeds, whereas *AtMan5-5* is predominantly expressed in the contracted endosperm of mature embryo green seeds (Fig. 7b). Finally, *AtMan5-2* is also highly expressed in the stem, and, similarly, the poplar single-gene *AtMan5-2* ortholog, POPTR_0013s13400, is highly expressed in xylem (Fig. 7c), suggesting that AtMan5-2 subclade genes are members of the secondary cell wall gene program.

To further investigate whether *At*Man5-2 subclade genes may be regulated by the secondary cell wall gene program, we examined if transcriptional cis-regulatory motifs in secondary cell wall synthesis are conserved in their upstream regions, since uncovering conserved cis-element motifs through bioinformatics allows elucidation of regulatory networks [59]. We focused on three cis-elements that mediate gene transactivation by transcription factors with well-established roles in secondary cell wall formation in the xylem: secondary wall NAC binding element (SNBE; [60]), which is bound by the NAC-type transcription factors NST1, SND1 and VND7; tracheary element-regulating *cis*-element (TERE; [61]), which is a possible binding site of VND7; and the AC-element as

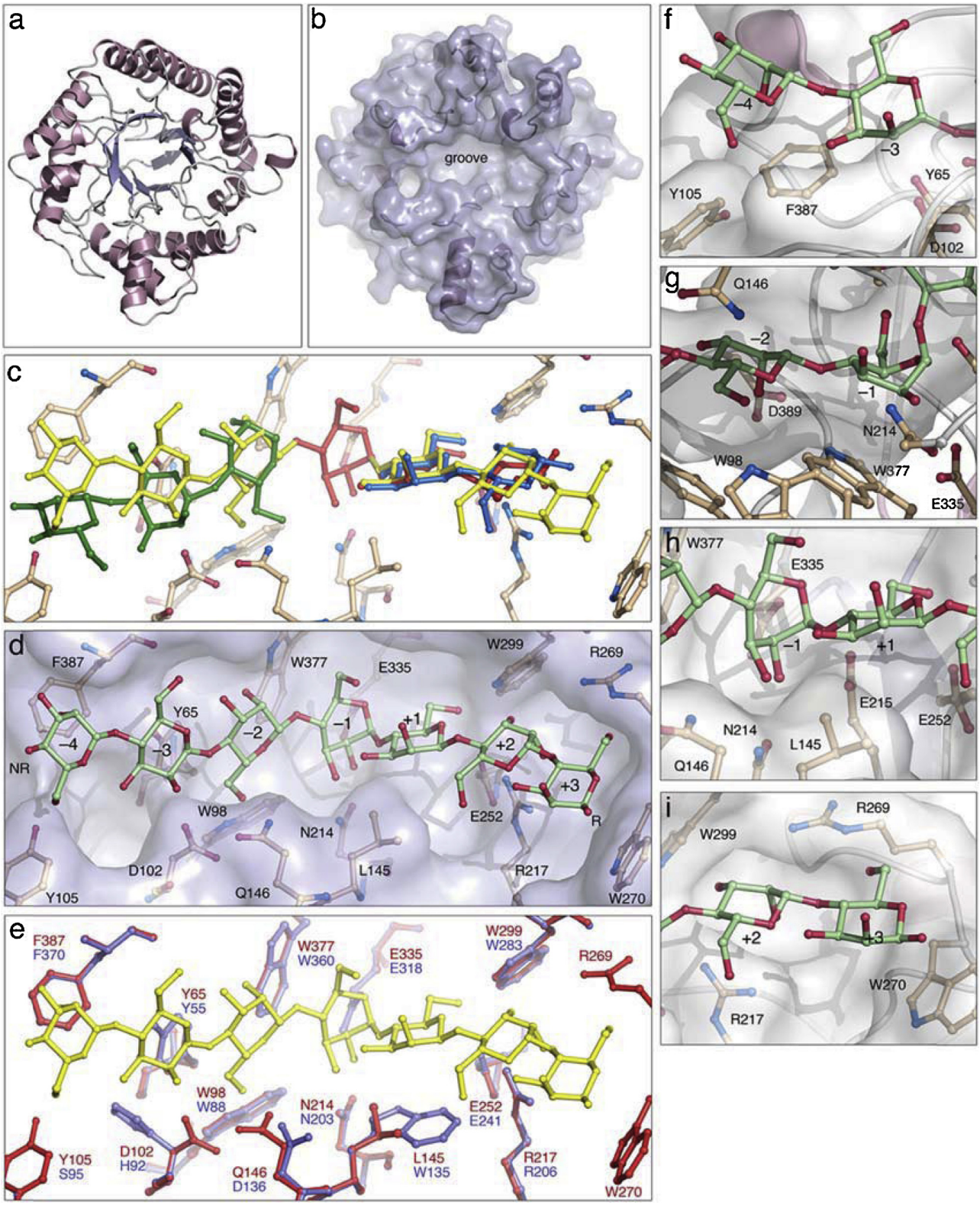

Fig. 6. (a) Ribbon representation of the *At*Man5-2 homology model generated by *SWISS-MODEL* (α-helices are shown in pink, β-strands in blue and loops in white). (b) Semitransparent molecular surface that highlights the groove that runs across the protein molecule (same view as in panel *a*). (c) Close-up view of the mannoheptaose (yellow) modeled in *At*Man5-2 across the groove. The docked mannoheptaose molecule is superimposed on the parental oligosaccharides from crystal-structure complexes: mannobiose (blue) in +1 to +2 from *Tr*Man5A (PDB code 1QNR; [40]); mannotriose (red) in –1 to +2 from *Rm*Man5B (PDB code 4LYQ; [41]); and mannotriose (green) in –4 to –2 from *Tf*Man (PDB code 3MAN; [42]). (d) The mannoheptaose molecule (green) with individual subsites numbered from the aglycone end (–4) to the glycone end (+3). The non-reducing and reducing end of the oligosaccharide is denoted NR and R, respectively. Relevant protein side chains are shown. (e) Overlay of the structure template *Le*MAN4a (blue; PDB code 1RH9) with the *At*Man5-2 model (red), and the docked mannoheptaose molecule (yellow) across the groove. (f)–(i) Details of the individual subsites proposed in panel *d*: (f) subsites –4 and –3; (g) subsites –2 and –1; (h) subsites –1 and +1; (i) subsites +2 and +3.

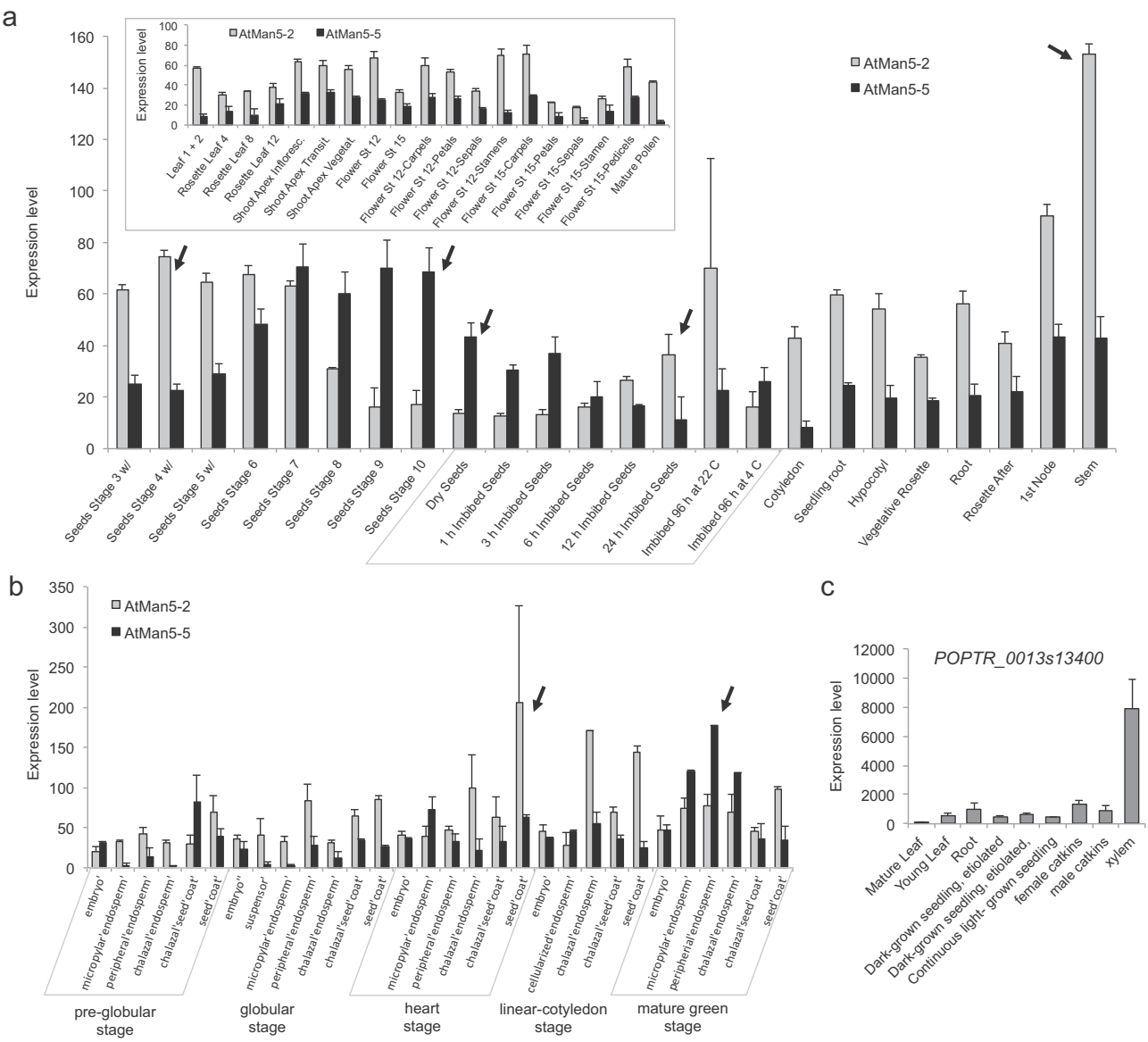

Fig. 7. Expression of *AtMan5-2* and *AtMan5-5*, and of the poplar ortholog POPTR_0013s13400. Values were obtained from the BAR eFP microarray database. (a) Expression levels of *AtMan5-2* (AT2G20680) and *AtMan5-5* (At4g28320) during the Arabidopsis life cycle. Seeds stage 3–5 are with siliques. (b) Expression levels of *AtMan5-2* (AT2G20680) and *AtMan5-5* (At4g28320) in tissues of the seed. (c) Expression levels of POPTR_0013s13400 in poplar tissues.

recently defined by Ratke et al. [62], which is the binding site of the transcription factor MYB46. Using MEME, a particular variant of the SNBE motif that is strikingly conserved in dicot *At*Man5-2 subclade genes (Table 2) was identified. Although several (ten out of 27) species lack this SNBE variant, they display other variants of the SNBE (not shown), and thus SNBE motifs are highly conserved in *At*Man5-2 subclade genes. The analysis also established that the AC motif is present in the proximal promoter region (700 bp from ATG) in 21 out of 27 dicot species (Supplementary Table S1). In contrast, the TERE motif, which is related to tracheary element programed cell death [61] is not conserved in Man5-2 genes. These results suggest that expression in the xylem is a conserved feature of *At*Man5-2 subclade genes in dicots.

However, *At*Man5-2 subclade genes are not strictly xylem-specific, as they are also expressed in seed tissues. In the developing seed, the high expression of *AtMan5-2* in the heart-stage embryo seed coat is coincident with mucilage production [63], suggesting a role for *At*Man5-2 in seed coat mucilage formation, whereas the high expression of *AtMan5-5* in the contracted endosperm suggests its involvement in endosperm hydrolysis. Consistent with this, knockout of *AtMan5-5* delays germination time, whereas knockout of *AtMan5-2* does not [31]. Glucomannan, which is the preferred substrate for *At*Man5-2, has been identified in the seed mucilage [12], and also in the Arabidopsis stem [8]. Thus, a possible biological function of the two *At*Man5-2-cluster enzymes may be to catalyze glucomannan hydrolysis in these tissues, but whether the activity is required for structural remodeling of the cell wall, or for generating manno-oligosaccharides as signal molecules, or both, cannot be concluded from the present data.

It is intriguing that genes coding for *At*Man5-2 cluster enzymes have undergone a gene duplication event early in *Brassicacea* evolution, and that the two genes display opposing gene expression patterns in seed tissues. Here, *AtMan5-2* and *AtMan5-5* could possibly participate in bidirectional cross-talk between seed coat and endosperm, a process where these two tissues mutually affect each other's development (reviewed by [64]). However, no seed coat phenotype was reported in knockout studies of *AtMan5-2* and *AtMan5-5* [31], so such possibility should necessarily involve redundant functions in other genes.

Table 2
An SNBE-like motif is conserved in dicot Man5-2 genes.

Gene name	Strand	Pos*	Sequence
Mesculenta_cassava4.1_027705m	+	−571	AGAATATTATATTTGAAGGAAGT
Mesculenta_cassava4.1_008068m	+	−551	AGAATATTAGAATTGAAGGAAAC
Rcommunis_29983.t000084	+	−587	GAAATATTAAAAAAGAAGGAACA
Lusitatissimum_Lus10033687.g	+	−187	GGAGCATTAATTTCCAAGAAACC
Lusitatissimum_Lus10031650.g	+	−186	GGAGCATTAATTTCCAAGAAACC
Lusitatissimum_Lus10039833.g	+	−268	GAAATATTAAATTTCAAGATATC
Lusitatissimum_Lus10018598.g	+	−241	AGAATATTAAATTTGAAGATATC
Ptrichocarpa_Potri.013G130400	+	−588	AGAATATTGAATTTGAAGAAACA
Pvulgaris_Phvul.011G118900	+	−544	AAAGTATTAGAACTGAAGGAAGG
Gmax_v1.1_Glyma12g12770	+	−552	AAAGTATTATAACTGAAGGGAGG
Gmax_v1.1_Glyma06g44750	+	−572	GTATTATTACAACTGAAGGAAGC
Ppersica_ppa005783m.g	+	−544	CAAATAGTAAACATGAAGAAAAG
Mdomestica_MDP0000709705	+	−525	GAAATATTAAAATTCAAGAAAAG
Mdomestica_MDP0000417632	+	−546	GAAATATTAAAATTCAAGAAAAG
Fvesca_gene17714-v1.0-hybrid	+	−413	CCAATATTAAACTCCAAGAAAAC
Brapa_Chifu401_v1.2_Bra031137	−	−628	CAAAAATTAAAATCTAAGCAAAG
Graimondii_Gorai.013G075700	+	−433	GATATATTAAATTTGAAGGAAAC
Graimondii_Gorai.005G201100	+	−375	GCTATATTAAAATTCAAGGAAAC
Tcacao_Thecc1EG008116	+	−361	GCTATATTAAAATTCAAGGAAAC
Csinensis_orange1.1g014151m.g	−	−60	AAAGAATTAAAACAGAAGACAAC
Csinensis_orange1.1g014151m.g	−	−525	AAAGCAGTCAAAAACAAGGGAGG
Cclementina_Ciclev10015394m.g	−	−59	AAAGAATTAAAACAGAAGACAAC
Cclementina_Ciclev10015394m.g	−	−527	AAAGCAGTCAAAAACAAGGGAGG
Egrandis_Eucgr.A01823	+	−709	AAAACATTGTAACTCAAGCAAAA
Vvinifera_GSVIVG01020553001	+	−628	AGATTATTAAAATTGAAGAAAAA
Mguttatus_v1.1_mgv1a007803m.g	−	−366	CAAGAATTAGTTATGAAGACAGC
CONSENSUS			ANNATTANANNNNAAGNNA T G G T C
SNBE	−		TNNCTTNNNNNNNAAGNAA A TC C CT G T

*Indicates distance in bp to translational start.

4. Conclusions

The Arabidopsis β-1,4-mannanase *At*Man5-2 represents a previously uncharacterized subclade of plant GH5_7 clade-1 MANs. Compared with the previously characterized Arabidopsis *At*Man5-1, *At*Man5-2 shows distinct kinetics, substrate preference, and hydrolysis-product patterns demonstrating catalytic diversification of plant MANs within one single plant species. Furthermore, no transglycosylation activity for *At*Man5-2 was observed in the present investigation. The enzyme displays the highest catalytic activity for mannan substrates containing glucose in the backbone, and is thus the first plant MAN with a preference for glucomannans. Results from oligomeric state analyses under non-reducing conditions suggest that *At*Man5-2 mainly is a monomer, although dimerization is possible. In particular one C-terminal Cys that is conserved in sequences of the *At*Man5-2 subclade appears suitable for disulfide-mediated dimerization. Results from sequence analysis and homology modeling suggest that the *At*Man5-2 substrate-binding cleft can accommodate seven sugar-binding subsites, −4 to +3, and shows that the *At*Man5-2 subclade has a leucine in subsite +1, which in other GH5 MANs is occupied by a sugar-stacking tryptophan side chain. Possibly, this leucine side chains weakens the interactions in subsite +1 to prevent transglycosylation. The demonstrated catalytic properties combined with analysis of gene expression data and conserved promoter motifs suggest a role for *At*Man5-2 in glucomannan regulation in the stem and seed coat mucilage.

Acknowledgements

HA acknowledges an Ingvar Carlsson Award from the Swedish Foundation for Strategic Research, and the Swedish Research Council Formas for financial support. CD acknowledges grants from the Swedish Research Councils VR and Formas. IE acknowledges a grant from the Swedish Governmental Agency for Innovation Systems VINNOVA. The authors are grateful to Dr. Chunlin Xu for providing the spruce galactoglucomannan.

Appendix A. Supplementary data

Supplementary data associated with this article can be found, in the online version, at http://dx.doi.org/10.1016/j.plantsci.2015.10.002.

References

[1] J.P. Zhuang, J. Su, W.X. Chen, Molecular cloning and characterization of fruit softening related gene β-mannanase from banana fruit, Agric. Sci. China 5 (2006) 277–283.
[2] M.S. Buckeridge, Seed cell wall storage polysaccharides: models to understand cell wall biosynthesis and degradation, Plant Physiol. 154 (2010) 1017–1023.
[3] M. Montiel, J. Rodríguez, M. Pérez-Leblic, M. Hernández, M. Arias, J. Copa-Patiño, Screening of mannanases in actinomycetes and their potential application in the biobleaching of pine kraft pulps, Appl. Microbiol. Biotechnol. 52 (1999) 240–245.
[4] J. Pang, Y.J. Sun, Y. Zhuang, B.H. Ye, Y.M. Sun, Dynamics study of the influence of temperature on konjac glucomannan saline solution's viscosity, Chinese J. Struct. Chem. 27 (2008) 394.
[5] M. Pauly, K. Keegstra, Plant cell wall polymers as precursors for biofuels, Curr. Opin. Plant Biol. 13 (2010) 304–311.
[6] L.R.S. Moreira, E.X.F. Filho, An overview of mannan structure and mannan-degrading enzyme systems, Appl. Microbiol. Biotechnol. 79 (2008) 165–178.
[7] B.V. McCleary, A.H. Clark, I. Dea, D.A. Rees, The fine structures of carob and guar galactomannans, Carbohydr. Res. 139 (1985) 237–260.
[8] M.G. Handford, T.C. Baldwin, F. Goubet, T.A. Prime, J. Miles, X. Yu, P. Dupree, Localisation and characterisation of cell wall mannan polysaccharides in *Arabidopsis thaliana*, Planta 218 (2003) 27–36.
[9] J.S. Kim, G. Daniel, Immunolocalization of hemicelluloses in *Arabidopsis thaliana* stem. Part II: mannan deposition is regulated by phase of development and its patterns of temporal and spatial distribution differ between cell types, Planta 236 (2012) 1367–1379.
[10] S.E. Marcus, A.W. Blake, T.A. Benians, K.J. Lee, C. Poyser, L. Donaldson, O. Leroux, A. Rogowski, H.L. Petersen, A. Boraston, H.J. Gilbert, W.G. Willats, J.P. Knox, Restricted access of proteins to mannan polysaccharides in intact plant cell walls, Plant J. 64 (2010) 191–203.
[11] I. Moller, I. Sørensen, A.J. Bernal, C. Blaukopf, K. Lee, J. Øbro, F. Pettolino, A. Roberts, J.D. Mikkelsen, J.P. Knox, A. Bacic, W.G. Willats, High-throughput mapping of cell-wall polymers within and between plants using novel microarrays, Plant J. 50 (2007) 1118–1128.
[12] L. Yu, D. Shi, J. Li, Y. Kong, Y. Yu, G. Chai, R. Hu, J. Wang, M.G. Hahn, G. Zhou, Cellulose synthase-like A2, a glucomannan synthase, is involved in maintaining adherent mucilage structure in Arabidopsis seed, Plant Physiol. 164 (2014) 1842–1856.
[13] F. Goubet, C.J. Barton, J.C. Mortimer, X. Yu, Z. Zhang, G.P. Miles, J. Richens, A.H. Liepman, K. Seffen, P. Dupree, Cell wall glucomannan in *Arabidopsis* is synthesised by CSLA glycosyltransferases, and influences the progression of embryogenesis, Plant J. 60 (2009) 527–538.
[14] K.J. Lee, B.J. Dekkers, T. Steinbrecher, C.T. Walsh, A. Bacic, L. Bentsink, G. Leubner-Metzger, J.P. Knox, Distinct cell wall architectures in seed endosperms in representatives of the Brassicaceae and Solanaceae, Plant Physiol. 160 (2012) 1551–1566.
[15] C. Rodríguez-Gacio Mdel, R. Iglesias-Fernández, P. Carbonero, A.J. Matilla, Softening-up mannan-rich cell walls, J. Exp. Bot. 63 (2012) 3976–3988.
[16] M. Couturier, M. Haon, P.M. Coutinho, B. Henrissat, L. Lesage-Meessen, J.G. Berrin, *Podospora anserina* hemicellulases potentiate the *Trichoderma reesei* secretome for saccharification of lignocellulosic biomass, Appl. Environ. Microbiol. 77 (2011) 237–246.
[17] P.S. Chauhan, N. Puri, P. Sharma, N. Gupta, Mannanases: microbial sources, production, properties and potential biotechnological applications, Appl. Microbiol. Biotechnol. 93 (2012) 1817–1830.
[18] V. Lombard, R.H. Golaconda, E. Drula, P.M. Coutinho, B. Henrissat, The carbohydrate-active enzymes database (CAZy) in 2013, Nucleic Acids Res. 42 (2014) D490–D495.
[19] D.E. Koshland Jr, Stereochemistry and the mechanism of enzymatic reactions, Biol. Rev. 28 (1953) 416–436.
[20] M.L. Sinnott, Catalytic mechanism of enzymic glycosyl transfer, Chem. Rev. 90 (1990) 1171–1202.
[21] M. Hrmova, R. Burton, P. Biely, J. Lahnstein, G. Fincher, Hydrolysis of (1,4)-beta-D-mannans in barley (*Hordeum vulgare* L.) is mediated by the concerted action of (1,4)-beta-D-mannan endohydrolase and beta-D-mannosidase, Biochem. J. 399 (2006) 77–90.
[22] A. Rosengren, S.K. Reddy, J.S. Sjöberg, O. Aurelius, D.T. Logan, K. Kolenová, H. Stålbrand, et al., An *Aspergillus nidulans* β-mannanase with high transglycosylation capacity revealed through comparative studies within

glycosidase family 5, Appl. Microbiol. Biotechnol. (2014), http://dx.doi.org/10.1007/s00253-014-5871-8.
[23] Y. Hakamada, Y. Ohkubo, S. Ohashi, Purification and characterization of β-mannanase from *Reinekea* sp. KIT-YO10 with transglycosylation activity, Biosci. Biotechnol. Biochem. 78 (2014) 722–728.
[24] R. Schroder, T.F. Wegrzyn, N.N. Sharma, R.G. Atkinson, LeMAN4 endo-beta-mannanase from ripe tomato fruit can act as a mannan transglycosylase or hydrolase, Planta 224 (2006) 1091–1102.
[25] Y. Wang, F. Vilaplana, H. Brumer, H. Aspeborg, Enzymatic characterization of a glycoside hydrolase family 5 subfamily 7 (GH5_7) mannanase from *Arabidopsis thaliana*, Planta 239 (2014) 653–665.
[26] R. Schröder, R.G. Atkinson, R.J. Redgwell, Re-interpreting the role of endo-beta-mannanases as mannan endotransglycosylase/hydrolases in the plant cell wall, Ann. Bot. 104 (2009) 197–204.
[27] H. Aspeborg, P.M. Coutinho, Y. Wang, H. Brumer, B. Henrissat, Evolution, substrate specificity and subfamily classification of glycoside hydrolase family 5 (GH5), BMC Evol. Biol. 12 (2012) 186.
[28] J.Y. Lin, V.R. Pantalone, G.L. Li, F. Chen, Molecular Cloning and biochemical characterization of an endo-beta-mannanase gene from soybean for soybean meal improvement, J. Agric. Food Chem. 59 (2011) 4622–4628.
[29] P. Marraccini, W.J. Rogers, C. Allard, M.L. André, V. Caillet, N. Lacoste, F. Lausanne, S. Michaux, Molecular and biochemical characterization of endo-beta-mannanases from germinating coffee (*Coffea arabica*) grains, Planta 213 (2001) 296–308.
[30] Y. Zhao, D. Song, J. Sun, L. Li, Populus endo-beta-mannanase PtrMAN6 plays a role in coordinating cell wall remodeling with suppression of secondary wall thickening through generation of oligosaccharide signals, Plant J. 74 (2013) 473–485.
[31] R. Iglesias-Fernandez, M.C. Rodríguez-Gacio, C. Barrero-Sicilia, P. Carbonero, A. Matilla, Three *endo*-β-mannanase genes expressed in the micropylar endosperm and in the radicle influence germination of *Arabidopsis thaliana* seeds, Planta 233 (2011) 25–36.
[32] M. Seki, P. Carninci, Y. Nishiyama, Y. Hayashizaki, K. Shinozaki, High-efficiency cloning of *Arabidopsis* full-length cDNA by biotinylated CAP trapper, Plant J. 15 (1998) 707–720.
[33] M. Seki, M. Narusaka, A. Kamiya, J. Ishida, M. Satou, T. Sakurai, M. Nakajima, A. Enju, K. Akiyama, Y. Oono, M. Muramatsu, Y. Hayashizaki, J. Kawai, P. Carninci, M. Itoh, Y. Ishii, T. Arakawa, K. Shibata, A. Shinagawa, K. Shinozaki, Functional annotation of a full-length *Arabidopsis* cDNA collection, Science 296 (2002) 141–145.
[34] M.M. Bradford, A rapid and sensitive method for the quantitation of microgram quantities of protein utilizing the principle of protein-dye binding, Anal. Biochem. 72 (1976) 248–254.
[35] G.L. Miller, Use of dinitrosalicylic acid reagent for determination of reducing sugar, Anal. Chem. 31 (1959) 426–428.
[36] J. Ma, S. Wang, F. Zhao, J. Xu, Protein threading using context-specific alignment potential, Bioinformatics 29 (2013) i257–i265.
[37] L.A. Kelley, M.J.E. Sternberg, Protein structure prediction on the web: a case study using the Phyre server, Nat. Protoc. 4 (2009) 363–371.
[38] M. Biasini, S. Bienert, A. Waterhouse, K. Arnold, G. Studer, T. Schmidt, F. Kiefer, T.G. Cassarino, M. Bertoni, L. Bordoli, T. Schwede, SWISS-MODEL: modelling protein tertiary and quaternary structure using evolutionary information, Nucleic Acids Res. 42 (2014) W252–W258.
[39] V.B. Chen, W.B. Arendall, J.J. Headd, D.A. Keedy, R.M. Immormino, G.J. Kapral, L.W. Murray, J.S. Richardson, D.C. Richardson, MolProbity: all-atom structure validation for macromolecular crystallography, Acta Crystallogr. D 66 (2010) 12–21.
[40] G. Vriend, C. Sander, Quality control of protein models: directional atomic contact analysis, J. Appl. Crystallogr. 26 (1993) 47–60.
[41] E. Sabini, H. Schubert, G. Murshudov, K.S. Wilson, M. Siika-Aho, M. Penttilä, The three-dimensional structure of a *Trichoderma reesei* beta-mannanase from glycoside hydrolase family 5, Acta Crystallogr. D 56 (2000) 3–13.
[42] P. Zhou, Y. Liu, Q. Yan, Z. Chen, Z. Qin, Z. Jiang, Structural insights into the substrate specificity and transglycosylation activity of a fungal glycoside hydrolase family 5 beta-mannosidase, Acta Crystallogr. D 70 (2014) 2970–2982.
[43] M. Hilge, S.M. Gloor, W. Rypniewski, O. Sauer, T.D. Heightman, W. Zimmermann, K. Winterhalter, K. Piontek, High-resolution native and complex structures of thermostable beta-mannanase from *Thermomonospora fusca*—substrate specificity in glycosyl hydrolase family 5, Structure 6 (1998) 1433–1444.
[44] D. Winter, B. Vinegar, H. Nahal, R. Ammar, G.V. Wilson, N.J. Provart, An electronic fluorescent pictograph browser for exploring and analyzing large-scale biological data sets, PLoS One 2 (2007) e718.
[45] O. Wilkins, H. Nahal, J. Foong, N.J. Provart, M.M. Campbell, Expansion and diver-sification of the populus R2R3-MYB family of transcription factors, Plant Physiol. 149 (2009) 981–993.
[46] T.L. Bailey, C. Elkan, Proceedings of the Second International Conference on Intelligent Systems for Molecular Biology, Menlo Park, California, 1994, pp. 28–36.
[47] Y. Zhao, Q. Zhang, L. Yuan, R. Zhang, L. Li, *N*-Glycosylation and dimerization regulate the PtrMAN6 enzyme activity that may modulate generation of oligosaccharide signals, Plant Signal. Behav. 8 (2013) e26956.
[48] Y. Kumagai, K. Kawakami, M. Uraji, T. Hatanaka, Binding of bivalent ions to actinomycete mannanase is accompanied by conformational change and is a key factor in its thermal stability, Biochim. Biophys. Acta 1834 (2013) 301–307.
[49] T. Nordahl Petersen, S. Brunak, G. von Heijne, H. Nielsen, SignalP 4.0: discriminating signal peptides from transmembrane regions, Nat. Methods 8 (2011) 785–786.
[50] L. Käll, A. Krogh, E.L.L. Sonnhammer, A combined transmembrane topology and signal peptide prediction method, J. Mol. Biol. 338 (2004) 1027–1036.
[51] A. Bernsel, H. Viklund, A. Hennerdal, A. Elofsson, TOPCONS: consensus prediction of membrane protein topology, Nucleic Acids Res. 37 (2009) W465–W468.
[52] R. Bourgault, A.J. Oakley, J.D. Bewley, W.C. Wilce, Three-dimensional structure of (1,4)-beta-D-mannan mannanohydrolase from tomato fruit, Protein Sci. 14 (2005) 1233–1241.
[53] F.M.V. Dias, F. Vincent, G. Pell, J.A.M. Prates, M.S.J. Centeno, L.E. Tailford, L.M.A. Ferreira, C.M.G.A. Fontes, G.J. Davies, H.J. Gilbert, Insights into the molecular determinants of substrate specificity in glycoside hydrolase family 5 revealed by the crystal structure and kinetics of *Cellvibrio mixtus* mannosidase 5A, J. Biol. Chem. 279 (2004) 25517–25526.
[54] L.E. Tailford, V.M. Ducros, J.E. Flint, S.M. Roberts, C. Morland, D.L. Zechel, N. Smith, M.E. Bjornvad, T.V. Borchert, K.S. Wilson, G.J. Davies, H.J. Gilbert, Understanding how diverse beta-mannanases recognize heterogeneous substrates, Biochemistry 48 (2009) 7009–7018.
[55] J.W. Huang, C.C. Chen, C.H. Huang, T.Y. Huang, T.H. Wu, Y.S. Cheng, T.P. Ko, C.Y. Lin, J.R. Liu, R.T. Guo, Improving the specific activity of β-mannanase from *Aspergillus niger* BK01 by structure-based rational design, Biochim. Biophys. Acta 1844 (2014) 663–669.
[56] A. Rosengren, P. Hägglund, L. Anderson, P. Pavon-Orozco, R. Peterson-Wulff, W. Nerinckx, H. Stålbrand, The role of subsite+ 2 of the *Trichoderma reesei* β-mannanase TrMan5A in hydrolysis and transglycosylation, Biocatal. Biotransform. 30 (2012) 338–352.
[57] S. Armand, S.R. Andrews, S.J. Charnock, H.J. Gilbert, Influence of the aglycone region of the substrate binding cleft of *Pseudomonas* xylanase 10A on catalysis, Biochemistry 40 (2001) 7404–7409.
[58] J.S. Yuan, X. Yang, J. Lai, H. Lin, Z.M. Cheng, H. Nonogaki, F. Chen, The endo-betamannanase gene families in *Arabidopsis*, rice, and poplar, Funct. Integr. Genomics 7 (2007) 1–16.
[59] Y. Pilpel, P. Sudarsanam, G.M. Church, Identifying regulatory networks by combinatorial analysis of promoter elements, Nat. Genet. 29 (2001) 153–159.
[60] R. Zhong, C. Lee, Z.H. Ye, Global analysis of direct targets of secondary wall NAC master switches in *Arabidopsis*, Mol. Plant 3 (2010) 1087–1103.
[61] H. Pyo, T. Demura, H. Fukuda, TERE; a novel cis-element responsible for a coordinated expression of genes related to programmed cell death and secondary wall formation during differentiation of tracheary elements, Plant J. 51 (2007) 955–965.
[62] C. Ratke, P.M. Pawar, V.K. Balasubramanian, M. Naumann, M.L. Duncranz, M. Derba-Maceluch, A. Gorzsás, S. Endo, I. Ezcurra, E.J. Mellerowicz, Populus GT43 family members group into distinct sets required for primary and secondary wall xylan biosynthesis and include useful promoters for wood modification, Plant Biotechnol. J. 13 (2015) 26–37.
[63] J.B. Windsor, V.V. Symonds, J. Mendenhall, A.M. Lloyd, *Arabidopsis* seed coat development: morphological differentiation of the outer integument, Plant J. 22 (2000) 483–493.
[64] D.D. Figueiredo, C. Köhler, Signalling events regulating seed coat development, Biochem. Soc. Trans. 42 (2014) 358–363.